Assessment of the indirect combustion noise generated in a transonic high-pressure turbine stage

By D. Papadogiannis†, G. Wang‡, S. Moreau‡, F. Nicoud¶, F. Duchaine†, L. Gicquel† AND J. W. Nichols‖

Indirect combustion noise, generated by the acceleration and distortion of entropy waves through the turbine stages, has been shown to be the dominant noise source of gas turbines at low frequencies and to impact the thermoacoustic behavior of the combustor. In the present work, indirect combustion noise generation is evaluated in the realistic, fully 3D transonic high-pressure turbine stage MT1 using Large-Eddy Simulations (LES). An analysis of the basic flow and the different turbine noise generation mechanisms is performed for two configurations: one with a steady inflow and one pulsed case, where a plane entropy wave train at a given frequency is injected at the inlet and propagates across the stage generating indirect noise. The noise is evaluated through the Dynamic Mode Decomposition (DMD) of the flow field. It is compared with previous 2D simulations of a similar stator/rotor configuration, as well as with the compact theory of Cumpsty & Marble (1977). Results show that the upstream propagating entropy noise is reduced due to the choked turbine nozzle guide vane. Downstream acoustic waves are found to be of similar strength as the 2D case, highlighting the potential impact of indirect combustion noise on the overall noise signature of the engine.

1. Introduction

Combustion noise is the low-frequency noise generated in the combustion chamber of gas turbines and comes from two main mechanisms. On the one hand, direct noise emanates from the acoustic waves created at the unsteady flame front and propagated through the rest of the engine at the speed of sound plus the convection velocity. On the other hand, the unsteady combustion also gives rise to low-frequency temperature fluctuations, or entropy waves. These waves are convected with the flow velocity to the combustor nozzle and turbine, where they are accelerated and distorted, generating acoustic waves. This is the indirect noise generation mechanism and its importance is twofold: first, it increases the noise signature of the engine and second, the acoustic waves propagating upstream can impact the thermoacoustic behavior of the combustion chamber (Motheau *et al.* 2014). Yet its actual relevance and relative importance with respect to the direct combustion noise remain controversial.

Due to the complexity of a full 3D high-pressure turbine, past theoretical and numerical studies of the phenomenon have used simplified turbine-like geometries. The first in-depth analyses on turbine-like geometries focused on the propagation of entropy waves

† CERFACS, France
‡ Université de Sherbrooke, Canada
¶ Université de Montpellier 2, France
‖ Department of Aerospace Engineering and Mechanics, University of Minnesota

through quasi-1D nozzles. Marble & Candel (1977) developed an analytical method to evaluate the transmission coefficients of acoustic and entropy waves propagating through a compact quasi-1D nozzle, its length being significantly smaller than the wavelength of the incoming waves. More recently, Duran & Moreau (2013) proposed an analytical method to calculate the transmission coefficients of general quasi-1D nozzles, removing the compact nozzle assumption. These analytical methods, accompanied by numerical predictions from LES, have been evaluated on the experimental Entropy Wave Generator (Bake *et al.* 2009), with Leyko (2010) reporting good agreement.

The theory of Marble and Candel for nozzles was extended to 2D compact blade rows by Cumpsty & Marble (1977), accounting for the turning of the flow. This was achieved by imposing an additional constraint, the Kutta condition at the blade trailing edge. The method, originally conceived for a single blade row, was extended to multistage turbines by Duran & Moreau (2012) and was compared against simulations of a 2D high-pressure turbine stage.

The present work is the first numerical evaluation of the indirect combustion noise generated in a realistic, fully 3D, transonic high-pressure turbine. A train of sinusoidal entropy waves of constant frequency and amplitude is injected to model the entropy waves generated in a combustor. For this study, the Dynamic Mode Decomposition (DMD) is employed for the analysis of the complex flow field (Schmid 2010).

2. Numerical set-up

The transonic MT1 turbine stage, consisting of 32 stator and 60 rotor blades, is chosen for this study. In an effort to find a reduced periodic domain for the simulations and control the computational cost, the reduced blade count technique is employed (Beard *et al.* 2011). It results in a domain with 1 stator blade and 2 rotors (12 degree periodicity), for which the mean predicted aerodynamic flow field has already been extensively validated against experimental measurements (Papadogiannis *et al.* 2014).

2.1. *Numerical schemes*

Performing LES of turbomachinery stages requires careful treatment of the rotor/stator interactions. To this end, the Multi Instances Solvers Coupled via Overlapping Grids (MISCOG) overset grid method is employed (Wang *et al.* 2014), where two instances of the reactive LES solver AVBP are coupled through the OpenPALM coupling software. The first instance computes the flow field across the stator, while the second one handles the moving blades of the turbine. The numerical scheme employed for all simulations is the two-step, finite-element TTGC (Colin & Rudgyard 2000) with explicit temporal integration, which is 3^{rd} order in time and space. This scheme is used in conjunction with Hermitian interpolation for the data exchange at the overlap zone, ensuring low dissipation and low dispersion of the rotor/stator interactions, while preserving the global order of accuracy of the employed numerical scheme.

2.2. *Mesh and Modeling*

A fully 3D hybrid mesh is used, with 10 prismatic layers around the blades and tetrahedral elements in the passage and endwalls. It is composed of 9.4 million cells in total for the stator domain and 21 million cells for the rotor domain. It is also designed to place the first nodes around the blade walls in the logarithmic region of a turbulent boundary layer. The cells closest to the wall have a maximum wall-normal separation of $\Delta y^+ = 50$. The prisms have a low aspect ratio set to $\Delta x^+ \approx \Delta z^+ \approx 4\Delta y^+$, allowing a good resolution

of streamwise/spanwise flow. The rotor tip region contains approximately 17 cell layers, yielding relatively limited resolution in that region but providing a reasonable time step. Subgrid-scale closure relies on WALE model (Nicoud & Ducros 1999).

2.3. *Boundary and operating conditions*

The boundary conditions follow the NSCBC formulation of Poinsot & Lele (1992). At the inlet the total temperature and total pressure are imposed, while at the outlet the static pressure is specified. Note that no turbulent fluctuations are added at the inlet, as only the pure indirect combustion noise generated in the turbine is investigated. For the forced simulations, sinusoidal entropy spots are introduced through the corresponding characteristic equation. The frequency of the imposed waves is 2kHz, corresponding to a wavelength equal to 0.4 the stator chord length at the turbine inlet, and the amplitude equal to 4.8% of the inlet total temperature. The operating and boundary conditions employed in this work are summarized in Table 1.

3. Results

In the following, the principal flow characteristics are identified for both a steady inflow and a forced case. Then, the global spectra of the forced case are investigated against those of the steady inflow case to evaluate the impact of the waves on the noise generation of the turbine. Afterwards, the response of the flow field at the pulsation frequency for the forced case is examined using DMD, and transmission coefficients are obtained for the generated acoustic waves. Finally, the results are compared to those obtained with the 2D theoretical model of Cumpsty & Marble (1977).

3.1. *Overall flow topology*

The overall flow topology is first analyzed for the two cases. Looking at the full 3D field, a particularly complex flow field is revealed. Figure 1 compares the density gradient of the flow across a cylindrical cut at the mid-span of the turbine for the steady inflow and pulsed cases (Figure 1(a,b)) and at an x-normal plane near the rotor trailing edge for the steady inflow case (Figure 1(c)). Some of the phenomena highlighted in Figure 1 are the shock/boundary layer interaction on the suction side of both the stator and the rotor (positions A and B), vortex shedding from the trailing edge of the blades and the accompanying acoustic waves emitted (position C), as well as strong secondary flows developing at the endwalls (positions D and E). For the pulsed case, in Figure 1(b), in addition to the previously highlighted phenomena, the planar entropy waves approaching the stator are also evidenced (position F). As they go through the stator passages they get distorted and partially mixed by the blade wakes before being cut by the passing rotors. The mixing and the developing turbulence make the entropy waves less visible in the rotor domain.

3.2. *Dynamic mode decomposition of the LES flow field*

A frequency domain analysis is performed by applying the DMD to a set of instantaneous flow fields. This method has been selected here, compared with other frequency-domain methods, for its robustness and the resolution capabilities with only few periods per frequency of interest included in the signal. Additionally, the frequency of the computed modes does not need to be a multiple of the sampling frequency, and the method minimizes spectral leakage. To obtain converged and accurate turbulent statistics, especially

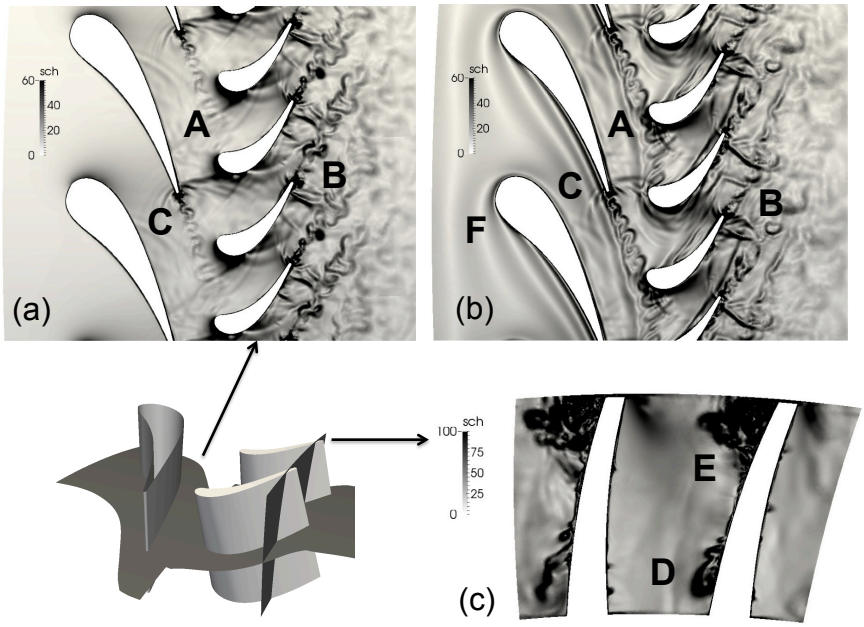

FIGURE 1. Contours $\|\nabla\rho|/\rho$ of an instantaneous solution at mid-span for the steady inflow (a) and pulsed cases (b). Contours of the same variable and at an x-normal plane near the rotor exit for the steady inflow case (c).

in the highly turbulent rotor-blade wake, both the steady inflow and the pulsed simulations ran for a total of 10 periods of the pulsation frequency. To avoid aliasing, the sampling frequency needs to be high enough to include all the important high-frequency phenomena. In this case the vortex shedding from the stator trailing edge is the most significant and resolving it, as well as its first harmonic, is necessary. The necessary sampling frequency was determined to be 120kHz using a simple fast fourier transform of a temporal signal recorded at a probe in the stator wake. Lower sampling frequencies were attempted (60kHz and 30kHz) but aliasing errors were present. Since DMD is memory consuming, the decomposition is performed at cylindrical blade-to-blade planes at mid-span with the signal including the six principal primitive variables: pressure, temperature, the three velocity components, and density. For the pulsed case, a set of x-normal planes at the inlet and outlet of the turbine stage is also employed to measure the incoming/outgoing acoustic and entropy waves as well as the transmission coefficients.

Figures 2 and 3 show, respectively, the DMD temperature and pressure spectra of the flow in the stator (left) and rotor (right) domains (azimuthal cuts) for the stationary and forced LES. For this configuration, the blade passing frequency (BPF) is 9.5kHz and 4.75kHz, respectively, for each domain. The depicted frequency ranges of Figures 2 and 3 cover up to a frequency equal to the BPF (as seen in each domain) plus the forced entropy wave frequency (EWF) at 2kHz. For the steady inflow case, Figures 2 and 3 reveal that there is no mode at the pulsation frequency. For the forced LES, pure entropy waves are injected, which create a distinctive peak in Figure 2, seen in both the stator and rotor domains. Furthermore, although no acoustic forcing is imposed by the entropy waves, Figure 3 reveals that a pressure mode with a distinctive peak appears. This indicates that acoustic waves have been generated, confirming the indirect noise

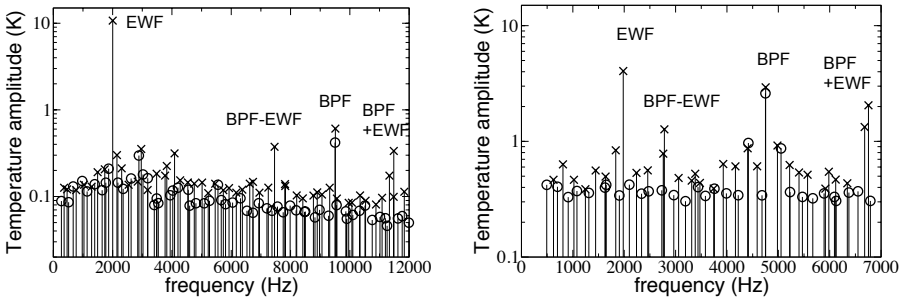

FIGURE 2. DMD temperature spectra of the stator (left) and rotor domain (right) at mid-span. Steady inflow case (○) and pulsed case (×).

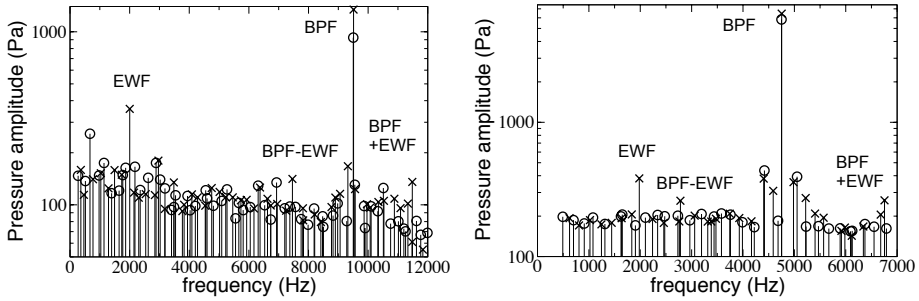

FIGURE 3. DMD pressure spectra of the stator (left) and rotor domain (right) at mid-span. Steady inflow case (○) and pulsed case (×).

generation mechanism. The imposed EWF also leads to the appearance of interaction modes between the BPF and this forcing, with noticeable pressure peaks arising at BPF ± EWF. This type of interaction between combustion noise and rotor/stator tones, yielding scattered tones, has also been measured on full-scale engine tests (Bennett & Fitzpatrick 2008).

The mode of primary interest obtained by DMD corresponds to the one at the EWF. Its spatial form can be visualized to identify the spatial activity at the origin of the EWF pressure peaks present in Figures 2 and 3. The modulus and phase of temperature, as well as pressure of the DMD mode are depicted in Figure 4 at mid-span. The temperature modulus at the inlet (Figure 4(a)) is practically uniform and equal to 20K, corresponding to the plane entropy waves injected in the domain. The phase at the same position (Figure 4(b)) indicates that the waves in this area are simply convected by the flow and stay planar. Downstream in the blade passage, the modulus gets distorted with a reducing maximum value, as was found in previous 2D propagation studies in a stator (Leyko 2010) and in a turbine stage (Duran & Moreau 2013). The phase also reveals an asymmetric distortion of the planar waves. This distortion is caused by the strong flow acceleration and turning imposed by the blades. An azimuthal component in the velocity is created, with the higher velocity near the suction side resulting in asymmetric propagation velocities across the azimuthal coordinate. In the rotor domain, due to the rotation, the blades see rather uniform entropy waves, with the phase at the rotor inlet being practically planar and perpendicular to the axial direction. As these waves pass through the rotors, they get deformed in a fashion similar to that in the first blade row. Such strong distortions of the injected entropy wave at both the stator and the rotor

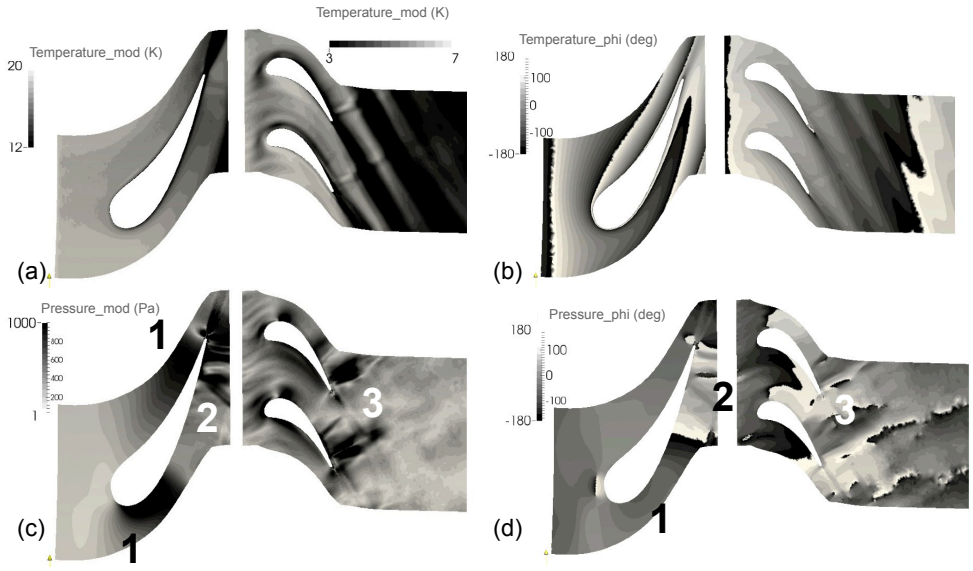

FIGURE 4. DMD 2kHz mode at mid-span - Modulus and phase of the temperature (a and b) and pressure (c and d) respectively.

leads to scattering in additional azimuthal modes. This energy redistribution mechanism can explain the additional peaks observed in the pressure and temperature spectra of Figures 2 and 3.

As anticipated in the discussion based on Figures 3 and 4, convected temperature spots produce pressure waves in both blade rows at the forcing frequency. The pressure modulus and the phase of the DMD mode at EWF, featured in Figures 4(c,d), reveal a complex pressure field. A significant peak of the modulus exists between the suction side at 20% chord length and the trailing edge on the pressure side, as the domain is periodic in the azimuthal direction (position 1). In this area the phase hardly changes (Figure 4(d)), suggesting an excited cavity mode that stays confined between the blades, rendering it irrelevant to combustion noise. The second area of high-pressure modulus can be observed on the suction side close to the trailing edge (position 2), with the sharpest peak corresponding to a shock. In the rotor domain, both the pressure modulus and phase appear to simply follow the flow, with a smooth change of phase throughout, indicating simple wave propagation. To finish, a large peak in the modulus at the trailing edge of the blade corresponds to another trailing edge shock (position 3). At the outlet, the acceleration of the temperature spots through the rotor and the acoustic waves generated in the stator and transmitted in the rotor are strong enough to yield a significant pressure trace (non-zero modulus) that sticks above the broadband level. All these features identified in the stator and rotor domains are at the root of the indirect combustion noise emitted and will be quantified later in this work.

3.3. *Sparsity-promoting dynamic mode decomposition*

The spectra of Figures 2 and 3 reveal that several other modes are also present around the EWF, and it is desirable to evaluate the most important contributions in terms of noise generation. To do so automatically, Jovanovic *et al.* (2014) developed a modified version of the DMD, called the sparsity-promoting DMD (SPDMD). It aims at selecting the

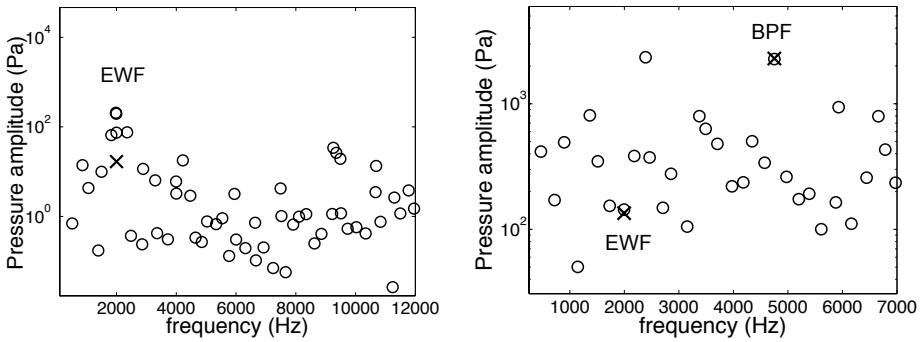

FIGURE 5. Sparsity-promoting DMD at the stator inlet (left) and rotor outlet (right) - Original DMD modes (∘) and SPDMD selected modes (×).

long-standing coherent modes that generate noise and remove the fast-decaying modes. This is achieved by a user-defined regularization parameter that controls the balance between accuracy and the number of modes retained.

In the following, the SPDMD is performed on pressure using the same set of instantaneous flow fields as in the previous sections, in order to identify the most important noise-generating modes of the flow. Figure 5 depicts the original pressure DMD spectrum with all the modes present complemented by the sparsity-promoting spectrum superimposed for the turbine inlet and outlet, respectively. Both diagnostics provided in Figure 5 are measured at the x-normal inlet and outlet planes for the pulsed case, as it is where the combustion noise will be measured. It can be seen that at the stator inlet the algorithm keeps only the pulsation mode, as expected. At the rotor exit, even though many more modes exist (caused by the local high-turbulence levels), the mode corresponding to the BPF and the pulsation frequency are chosen as the most coherent. It can further be noted that the algorithm retains this 2kHz mode, despite its weak amplitude. This result serves to highlight the importance of the indirect combustion noise with respect to other flow phenomena. It also shows that the SPDMD can be an appealing method for the analysis of combustors, as it has the potential to quickly identify the entropy modes that are most probable to generate indirect noise.

3.4. *Quantifying the indirect noise and comparisons with the compact theory*

The noise that is measured in this study is the result of a pulsated, realistic 3D turbine involving complex interactions between different flow physics and with several technological effects present (notably, the secondary flows at the hub and casing of the stator, the tip leakage flow at the rotor, the complete 3D shock structures, and the shock-boundary layer interactions). It can be compared with the 2D compact theory of Cumpsty & Marble (1977). Numerical results from 2D simulations of a simplified turbine stage published by Duran & Moreau (2013) can serve as an additional complement to the theory and the full 3D simulations. Indeed, Duran & Moreau (2013) commented that 2kHz is approximately the frequency limit after which the compact assumption is not valid.

To measure the transmission of the generated acoustic waves, DMD is performed at the inlet and outlet x-normal planes. Assuming that at these locations the dimensionless waves are 1D plane waves, the downstream propagating acoustic wave can be calculated as $w^+ = p'/\gamma\overline{p} + u'/\overline{c}$, the upstream propagating acoustic wave as $w^- = p'/\gamma\overline{p} - u'/\overline{c}$ and the entropy wave $w^s = p'/\gamma\overline{p} - \rho'/\overline{\rho}$. The overline in these expressions indicates

time-averaged quantities, the prime indicates fluctuations, and the heat capacity ratio γ is assumed to be constant throughout, while u indicates the axial component of the velocity. The transmission coefficients of interest are the entropy wave attenuation $Ts = w_2^s/w_1^s$, the acoustic wave reflection $Ra = w_1^-/w_1^s$ and the acoustic wave transmission $Tr = w_2^+/w_1^s$, with the subscript 1 indicating the turbine inlet, the subscript 2 referring to the turbine outlet, and w_1^s being the entropy waves imposed at the inlet.

The procedure to construct the characteristic waves and measure the transmission coefficients at the inlet and outlet of the turbine stage can be decomposed into 5 steps: (i) Perform DMD of the principal flow variables at an x-normal plane both at the inlet and outlet of the turbine. (ii) Isolate the mode of interest (2kHz in this case) and form the temporal fluctuations of the variables. (iii) For each point in the plane construct the 1D plane waves using the reconstructed fluctuations and a time-averaged solution. (iv) Perform surface averaging and calculate the transmission coefficients.

Applying this procedure at the inlet of the turbine stage is straightforward, since there is no free-stream turbulence imposed. However, as the flow goes through the turbine it generates broadband fluctuations. While DMD allows an easy filtering of all irrelevant frequencies, turbulence or hydrodynamic phenomena whose frequency coincides with the pulsation frequency will be present in the signal and can therefore modify the evaluation of the transmission coefficients. As a result, at the rotor outlet an extra step is added before step (iv): a hydrodynamic filtering based on the characteristics based filtering (CBF) method (Kopitz *et al.* 2005) is applied to separate hydrodynamics from acoustics using their known propagation velocities. To apply this filtering, the waves are measured in 3 outlet x-normal planes (instead of just 1) in close proximity. The Taylor hypothesis and the known acoustic convection velocity are then used to correlate the data between the 3 planes from different physical times following the formula

$$w_a = \frac{1}{3}\sum_{i=0}^{2} f(x - i\Delta x, t - \frac{i\Delta x}{u_p}). \tag{3.1}$$

In Eq. (3.1), f is the wave of interest, w_a is the filtered wave, Δx is the distance between the planes, and u_p is the convection velocity of the wave.

Results, applying the procedure described above, are summarized in Table 2, where they are also compared to the theory and 2D numerical predictions. Regarding the entropy wave attenuation, the results of the 3D simulation suggest that at the turbine outlet the injected wave has been dissipated more than in the 2D simulations, while the theoretical approach neglects completely the entropy wave attenuation process. Regarding the acoustic wave transmission, the 2 numerical simulations are in reasonable agreement, highlighting that the combustion noise levels remain similar. For the acoustic wave reflection (upstream propagating acoustic waves), the 3D simulation predicts a small decrease in strength compared to the 2D prediction, probably because of the choked operating condition that prevents acoustic waves generated downstream of the sonic line to propagate towards the turbine inlet.

4. Conclusions

The indirect combustion noise generation has been evaluated with LES of a 3D high-pressure turbine stage subjected to a constant-frequency entropy wave train pulsation. To simplify the data processing, the flow field and the generated noise are analyzed through the DMD of instantaneous snapshots at several positions across the turbine and

Rotational Speed (rpm)	9500
Inlet total pressure (Pa)	$4.56e5$
Inlet total temperature (K)	444
Mass flow (kg/sec)	17.4
Outlet static pressure (Pa)	$1.4e5$
Wave amplitude (K)	20
Wave frequency (Hz)	2000

TABLE 1. Operating conditions of the MT1 turbine

	3D LES	2D LES	Theory
Ts	0.09	0.3	1
Tr	0.017	$0.018 - 0.02$	0.015
Ra	0.018	0.025	0.07

TABLE 2. Summary of the transmission coefficients

the results are compared with a steady inflow case. Entropy wave injection generates a distinctive high-amplitude mode at the pulsation frequency, as well as interaction modes with the blade passing frequency. The influence of the entropy waves is also captured by the SPDMD, a modified DMD algorithm that provides an accurate reconstruction of the flow field with only few of the most coherent modes. Despite the presence of broadband turbulence and non-linear interactions, the blade passing frequency and pulsation modes are shown to be the most important. For the forced frequency, a detailed analysis of the 3D LES predictions is performed and the results are compared with the compact theory of Cumpsty & Marble (1977) as well as 2D simulations of a similar turbine configuration. While the compact theory overpredicts the noise levels, the 3D LES of the choked transonic HP turbine reveals that the entropy waves become highly distorted. The 3D entropy waves are transmitted even less efficiently to downstream stages than 2D simulations and the compact theory and thus are unlikely to generate any additional indirect noise; the transmitted acoustic waves, however, remain strong and contribute to the indirect noise as in 2D. The reflected acoustic waves are slightly weaker than in 2D and far less than in the compact theory, and will therefore not amplify any potential acoustic instabilities in the combustion chamber.

Acknowledgments

The authors would like to thank Prof. Peter Schmid for fruitful discussions and suggestions on the DMD. The help of Dr. Marlene Sanjosé, Thomas Jaravel, Thomas Livebardon and Michael Bauerheim is gratefully acknowledged. This work was performed using HPC resources from GENCI- [TGCC/CINES/IDRIS] (Grant 2014-x20142b5031) and from Compute Canada.

REFERENCES

BAKE, F., RICHTER, C., MUHLBAUER, B., KINGS, N., I.ROHLE, F.THIELE & B.NOLL 2009 The entropy wave generator: a reference case on entropy noise. *J. Sound Vib.* pp. 574–598.

BEARD, P., SMITH, A. & POVEY, T. 2011 Experimental and computational fluid dynamics investigation of the efficiency of an unshrouded transonic high pressure turbine. *J. Power Energy* **225**, 1166–1179.

BENNETT, G. & FITZPATRICK, J. 2008 Noise source identification for ducted fan systems. *AIAA Journal* **46**, 1663–1674.

COLIN, O. & RUDGYARD, M. 2000 Development of high-order Taylor-Galerkin schemes for unsteady calculations. *J. Comput. Phys.* **162**, 338–371.

Cumpsty, N. A. & Marble, F. E. 1977 The interaction of entropy fluctuations with turbine blade rows; a mechanism of turbojet engine noise. *Proc. R. Soc. Lond. A* **357**, 323–344.

Duran, I. & Moreau, S. 2012 Study of the attenuation of waves propagating through fixed and rotating turbine blades. In *18th AIAA/CEAS Aeroacoustics Conference*, pp. AIAA2012–2133.

Duran, I. & Moreau, S. 2013 Solution of the quasi one-dimensional linearized euler equations using flow invariants and the magnus expansion. *J. Fluid Mech.* **723**, 190–231.

Jovanovic, M. R., Schmid, P. & Nichols, J. 2014 Sparsity-promoting dynamic mode decomposition. *Phys. Fluids* **26**, 024103.

Kopitz, J., Bröcker, E. & Polifke, W. 2005 Characteristics-based filter for identification of planar acoustic waves in numerical simulation of turbulent compressible flow. In *Proc. 12th ICSV.*

Leyko, M. 2010 *Mise en oeuvre et analyse de calculs aéroacoustiques de type LES pour la prévision du bruit de chambres de combustion aéronautiques.* PhD thesis, Institut National Polytechnique de Toulouse.

Marble, F. E. & Candel, S. 1977 Acoustic disturbances from gas nonuniformities convected through a nozzle. *J. Sound Vib.* **55**, 225–243.

Motheau, E., Selle, L., Poinsot, T. & Nicoud, F. 2014 Mixed acoustic-entropy combustion instabilities in gas turbines. *J. Fluid Mech.* **749**, 542–576.

Nicoud, F. & Ducros, F. 1999 Subgrid-scale modelling based on the square of the velocity gradient tensor. *Flow Turbul. Combust.* **62**, 183–200.

Papadogiannis, D., Wang, G., Moreau, S., Duchaine, F., Sicot, F. & Gicquel, L. 2014 Large eddy simulation of a high-pressure turbine stage: Effects of sub-grid scale modeling and mesh resolution. In *Proc. ASME Turbo Expo 2014*.

Poinsot, T. & Lele, S. 1992 Boundary conditions for direct simulations of compressible viscous flows. *J. Comput. Phys.* **101**, 104–129.

Schmid, P. 2010 Dynamic mode decomposition of numerical and experimental data. *J. Fluid Mech.* **656**, 5–28.

Wang, G., Duchaine, F., Papadogiannis, D., Duran, I., Moreau, S. & Gicquel, L. 2014 An overset grid method for large eddy simulation of turbomachinery stages. *J. Comput. Phys.* **274**, 333–355.